

The Coupled Response of Turbomachinery Blading to Aerodynamic Excitations

Daniel Hoyniak* and Sanford Fleeter†
Purdue University, West Lafayette, Indiana

An energy balance technique is developed which predicts the coupled bending torsion mode aerodynamic forced response of an airfoil. The effects of the various aerodynamic parameters are then considered utilizing a subsonic compressible flow/flat plate cascade gust analysis. The increased coupling between the torsion and translation modes as the natural frequencies approach one another is shown. It is also demonstrated that the coupled response amplitudes increase with: 1) decreased structural damping, 2) increased solidity, stagger angle, and Mach numbers, 3) interblade phase angles corresponding to forward traveling waves, and 4) shifting of the elastic axis location aft.

Nomenclature

a	= distance of elastic axis aft of mid chord
A	= unsteady lift influence coefficient
b	= airfoil semichord ($C/2$)
B	= unsteady moment influence coefficient
C	= airfoil chord
C/S	= cascade solidity (airfoil chord/airfoil spacing)
C_1	= $\mu x_\alpha + (A_\alpha)^R$
C_2	= $\mu x_\alpha + (B_h)^R$
C_3	= $[\mu - \mu(\omega_h/\bar{\omega})^2 + (A_h)^R]$
C_4	= $(A_h)^I - \mu(\omega_h/\bar{\omega})^2 g_h$
C_5	= $\mu r_\alpha^2 [1 - (\omega_\alpha/\bar{\omega})^2] + (B_\alpha)^R$
C_6	= $(B_\alpha)^I - \mu r_\alpha^2 (\omega_\alpha/\bar{\omega})^2 g_\alpha$
C_7	= $-(W_G/U)(A_G)^R$
C_8	= $-(W_G/U)(A_G)^I$
C_9	= $-(W_G/U)(B_G)^R$
C_{10}	= $-(W_G/U)(B_G)^I$
D_1	= $\{ (C_4 C_5 + C_6 C_3) - [C_2 (A_\alpha)^I + C_1 (A_h)^I] \}$
D_R	= $\{ (C_3 C_5 - C_4 C_6) - [C_2 C_1 - (A_\alpha)^I (B_h)^I] \}$
h	= complex translational displacement
h_0	= amplitude of translational oscillation
i	= $\sqrt{-1}$
I_α	= mass moment of inertia per unit span about the elastic axis
k	= reduced frequency ($k = \bar{\omega} b/U$)
L	= unsteady lift
m	= mass per unit span of the airfoil
M	= unsteady moment
N_{hI}	= $\{ (C_8 C_5 + C_6 C_7) - [C_9 (A_\alpha)^I + C_1 C_{10}] \}$
N_{hR}	= $\{ (C_7 C_5 - C_8 C_6) - [C_1 C_9 - C_{10} (A_\alpha)^I] \}$
$N_{\alpha I}$	= $\{ (C_{10} C_3 + C_4 C_9) - [C_7 (B_h)^I + C_2 C_8] \}$
$N_{\alpha R}$	= $\{ (C_3 C_9 - C_4 C_{10}) - [C_7 C_2 - C_8 (B_h)^I] \}$
$\text{Re}[\]$	= real part of $[\]$
r_α	= radius of gyration about elastic axis
S_α	= airfoil static moment per unit span about the elastic axis

U	= freestream velocity
W	= complex transverse gust function
W_G	= amplitude of transverse gust
WORK	= unsteady work per cycle of oscillation
x_α	= location of center of gravity relative to elastic axis
α	= complex torsional displacement
α_0	= amplitude of torsional motion
μ	= mass parameter
ρ	= fluid density
σ	= interblade phase angle
ω	= airfoil natural frequency
$\bar{\omega}$	= frequency of the transverse gust

Subscripts

G	= gust
h	= translation
SI	= self induced (aerodynamic damping)
α	= torsion

Superscripts

I	= imaginary part
R	= real part
$(\)$	= derivative with respect to time

Introduction

AERODYNAMICALLY induced vibrations of rotor and stator airfoils are one of the more common sources of high cycle fatigue failure in gas turbine engines. Destructive aerodynamic forced responses of fan compressor and turbine blading have been generated by a wide variety of sources including upstream blades and/or vanes distortion, rotating stall, downstream blades and/or vanes surge bleeds, and random or otherwise unidentified sources.

Failure level vibratory responses occur when a periodic aerodynamic forcing function with frequency equal to a natural blade resonant frequency acts on a blade row. The rotor speeds at which these forced responses occur are predicted with Campbell diagrams, which display the natural frequency of each blade mode vs rotor speed.¹ Whenever these curves cross, aerodynamically induced forced responses are possible. However, at the present time no accurate prediction for the amplitude of the resulting stress can be made.

The prediction of the aerodynamic forced response vibratory behavior of a blade or vane row requires a definition of the unsteady forcing function in terms of its harmonics. The time variant aerodynamic response of the

Presented as Paper 83-0844 at the AIAA/ASME/ASCE/AHS Structures, Structural Dynamics, and Materials Conference, Lake Tahoe, Nev., May 2-4, 1983; received May 13, 1983; revision received Oct. 3, 1983. Copyright © American Institute of Aeronautics and Astronautics, Inc., 1983. All rights reserved.

*Graduate Research Assistant; presently Aerospace Engineer, NASA Lewis Research Center, Cleveland, Ohio.

†Professor of Mechanical Engineering, and Director, Thermal Sciences and Propulsion Center, Member AIAA.

airfoil to each harmonic of this forcing function is then assumed to be comprised of two parts.² One part is due to the disturbance being swept past the non responding fixed airfoils. The second arises when the airfoils respond to this disturbance. These effects are modeled by means of two distinct analyses. A linearized small perturbation gust analysis is used to predict the time variant aerodynamics of the fixed non-responding airfoil to each harmonic of the disturbance. A self induced unsteady aerodynamic analysis wherein the airfoils are assumed to be harmonically oscillating, is then used to predict the additional aerodynamic effect due to the airfoil response. These self induced aerodynamic effects can be thought of as an aerodynamic damping which can be either positive or negative. Reviews of state of the art unsteady aerodynamics as applied to turbomachines, including gust and self induced unsteady aerodynamic analyses, are presented in Refs. 3 and 4.

The classical approach to the prediction of the aerodynamic forced response of an airfoil is based on Newton's second law. The gust and self induced unsteady aerodynamic analyses are used to describe the harmonic forces and moments acting on the airfoil in conjunction with a lumped parameter description of the airfoil structural and inertial properties.⁵

An alternate approach based on an energy balance technique has been developed by Hoyniak and Fleeter⁶ to predict the uncoupled single degree of freedom forced response of an airfoil. In this approach, a balance is established between the energy of unsteady aerodynamic work and the energy dissipated by the airfoil.

The objective of this paper is to extend the energy balance technique to include the more interesting case of coupled bending-torsion mode forced response of an airfoil and, also, to demonstrate the effects of the various aerodynamic and structural parameters on this coupled response.

General Unsteady Aerodynamic Coefficients

Figure 1 presents a schematic representation of a two dimensional airfoil section displaced in both torsion and translation in a uniform flow with a superimposed convected transverse sinusoidal gust. Equation (1) presents the complex time dependent unsteady lift and moment per unit span written in influence coefficient form for the gust response and the self induced unsteady aerodynamic cases.

$$\begin{aligned} L_G &= L_G^R + iL_G^I = \pi\rho b^2 \bar{\omega}^2 \left[A_G \left(\frac{W}{U} \right) \right] \\ M_G &= M_G^R + iM_G^I = \pi\rho b^4 \bar{\omega}^2 \left[B_G \left(\frac{W}{U} \right) \right] \\ L_{SI} &= L_{SI}^R + iL_{SI}^I = \pi\rho b^3 \omega^2 \left[A_h \frac{h}{b} + A_\alpha \alpha \right] \\ M_{SI} &= M_{SI}^R + iM_{SI}^I = \pi\rho b^4 \omega^2 \left[B_h \frac{h}{b} + B_\alpha \alpha \right] \end{aligned} \quad (1)$$

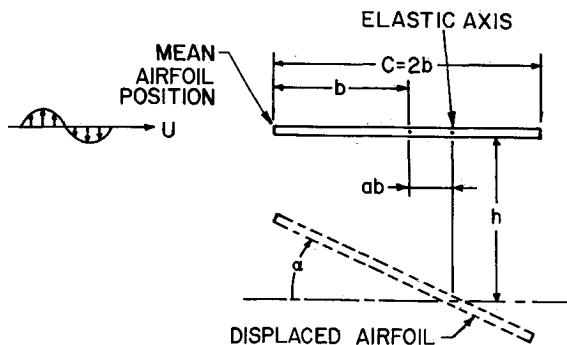


Fig 1 Airfoil and displacement geometry and notation

where $h = h_0 e^{i\omega t}$; $\alpha = \alpha_0 e^{i\omega t}$. $W = W_G e^{i\omega t}$ describes the gust; (A_h, B_h) , (A_α, B_α) , (A_G, B_G) denote the generalized unsteady lift and moment coefficients due to airfoil translation, airfoil torsion and the convected sinusoidal gust respectively; ω is the airfoil natural frequency and $\bar{\omega}$ is the gust forcing function frequency.

The total unsteady lift and moment on the airfoil are obtained by superimposing the gust response and the self induced aerodynamic forces and moments.

$$\begin{aligned} L(t) &= L_G(t) + L_{SI}(t) \\ &= \pi\rho b^2 \bar{\omega}^2 \left[A_G \left(\frac{W_G}{U} \right) + A_h h_0 + A_\alpha \alpha_0 \right] e^{i\omega t} \\ M(t) &= M_G(t) + M_{SI}(t) \\ &= \pi\rho b^4 \bar{\omega}^2 \left[B_G \left(\frac{W_G}{U} \right) + B_h h_0 + B_\alpha \alpha_0 \right] e^{i\omega t} \end{aligned} \quad (2)$$

It should be noted that the airfoil response occurs at the frequency of the forcing function. Hence, in Eq. (2) the gust frequency $\bar{\omega}$ has been utilized in the specification of the unsteady aerodynamic forces and moments.

Energy Balance

The equations of motion describing the coupled translational and torsional displacement of the flat plate airfoil depicted in Fig. 1 are given in Eq. (3).

$$\begin{aligned} m\ddot{h} + S_\alpha \ddot{\alpha} + m\omega_h^2 (1 + i g_h) h &= L(t) \\ S_\alpha \ddot{h} + I_\alpha \ddot{\alpha} + I_\alpha \omega_\alpha^2 (1 + i g_\alpha) \alpha &= M(t) \end{aligned} \quad (3)$$

where m denotes the mass per unit span of the airfoil. S_α is the airfoil static moment per unit span about the elastic axis. ω_h and ω_α are the translational and torsional mode airfoil natural frequencies of the corresponding undamped single degree of freedom system respectively and I_α is the mass moment of inertia per unit span about the elastic axis. As seen, the airfoil structural dynamic system described in Eq. (3) is strongly coupled and the coupling is associated with both the structural and the aerodynamic characteristics of the system. The structural coupling becomes significant whenever the aerodynamic center does not coincide with the elastic axis in which case a non-zero value for the airfoil static moment results. The aerodynamic coupling arises because the self induced aerodynamic forces acting on the airfoil are a function of the translational and torsional motions.

In this investigation, the coupled system response is determined utilizing an energy balance technique. The energy input to the system per cycle of airfoil oscillation is generated by the gust and, under certain conditions, the self induced unsteady aerodynamic forces and moments.⁶ The energy dissipation of the system per cycle is associated with 1) system structural damping, 2) under certain conditions the self induced aerodynamic forces and moments, and 3) the static moment term S_α . It should be noted that for the uncoupled single degree of freedom case, the dissipation term S_α was not considered.

The energy balance for the coupled translation-torsion airfoil motion can be expressed as follows:

$$\begin{aligned} (\text{WORK})_{SI}^h + (\text{WORK})_{gh}^h + (\text{WORK})_g^h &= (\text{WORK})_G^h \\ (\text{WORK})_{SI}^\alpha + (\text{WORK})_{g\alpha}^\alpha + (\text{WORK})_{S\alpha}^\alpha &= (\text{WORK})_G^\alpha \end{aligned} \quad (4)$$

where

$(\text{WORK})_{SI}^h (\text{WORK})_{SI}^g$ = work done by the self induced aerodynamic forces and moments in translation and torsion respectively

$(\text{WORK})_{gh}^h, (\text{WORK})_{g\alpha}^g$ = work done by the airfoil translation and torsion structural damping respectively

$(\text{WORK})_{S\alpha}^h (\text{WORK})_{S\alpha}^g$ = work associated with the static moment S_α in translation and torsion respectively

$(\text{WORK})_G^h (\text{WORK})_G^g$ = work done by the gust aerodynamic forces and moments in translation and torsion respectively

The work values associated with the self induced unsteady aerodynamic forces and moments, $(\text{WORK})_{SI}^h$ and $(\text{WORK})_{SI}^g$, have been written as dissipation terms. However under certain conditions they may actually represent energy input terms. The sign differentiates between energy dissipation and input. Also matrix techniques are utilized to solve Eq (4) in order to determine the response of the airfoil system.

The unsteady work done by the self induced aerodynamic terms $(\text{WORK})_{SI}^h$ and $(\text{WORK})_{SI}^g$ over one cycle of vibration can be calculated from Eq (5)

$$\begin{aligned} (\text{WORK})_{SI}^h &= \oint \text{Re}[L_{SI}(t) dh] \\ (\text{WORK})_{SI}^g &= \oint \text{Re}[M_{SI}(t) d\alpha] \end{aligned} \quad (5)$$

where $L_{SI}(t)$ and $M_{SI}(t)$ denote the unsteady lift and moment associated with the self induced harmonic motion of the airfoil [See Eq (1)]

Carrying out the integrations specified by Eqs 1 and 5 results in the following expressions for the unsteady work done by the self induced aerodynamic forces and moments

$$\begin{aligned} (\text{WORK})_{SI}^h &= \pi^2 \rho b^3 \bar{\omega}^2 [-(A_h)^1 h_0^2 / b + (A_\alpha)^R h_0 \alpha_0 \\ &\quad \times \sin(\lambda_h - \lambda_\alpha) - (A_\alpha)^1 h_0 \alpha_0 \cos(\lambda_h - \lambda_\alpha)] \\ (\text{WORK})_{SI}^g &= \pi^2 \rho b^4 \bar{\omega}^2 \left[(B_h)^R \left(\frac{h_0 \alpha_0}{b} \right) \sin(\lambda_h - \lambda_\alpha) \right. \\ &\quad \left. - (B_h)^1 \left(\frac{h_0 \alpha_0}{b} \right) \cos(\lambda_h - \lambda_\alpha) - (B_\alpha)^1 \alpha_0^2 \right] \end{aligned} \quad (6)$$

The angle λ_h denotes the phase angle between the incoming gust and the resulting translational motion of the airfoil. Similarly the angle λ_α is the phase angle between the incoming gust and the airfoil torsional motion.

The energy input to the airfoil is determined by calculating the work per cycle of oscillation of the unsteady lift and moment associated with the incoming gust

$$\begin{aligned} (\text{WORK})_G^h &= - \oint \text{Re}[L_G(t) dh] \\ &= -\pi \rho b^3 \bar{\omega}^2 h_0 [(A_G)^1 \cos(\lambda_h) - (A_G)^R \sin(\lambda_h)] \\ (\text{WORK})_G^g &= \oint \text{Re}[M_G(t) d\alpha] \\ &= \pi \rho b^4 \bar{\omega}^2 \alpha_0 [(B_G)^1 \cos(\lambda_\alpha) - (B_G)^R \sin(\lambda_\alpha)] \end{aligned} \quad (7)$$

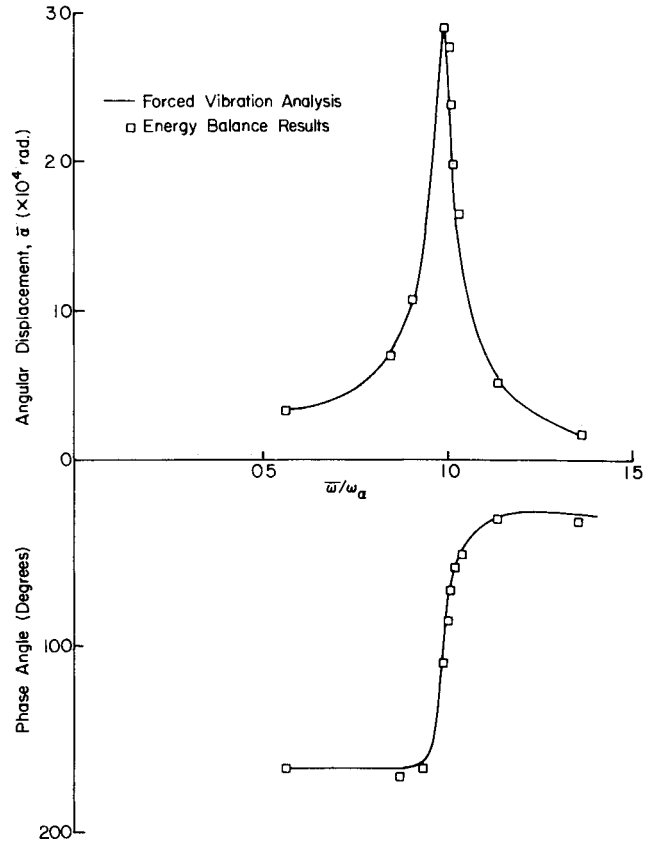


Fig 2 Comparison of classical and energy balance forced response calculations

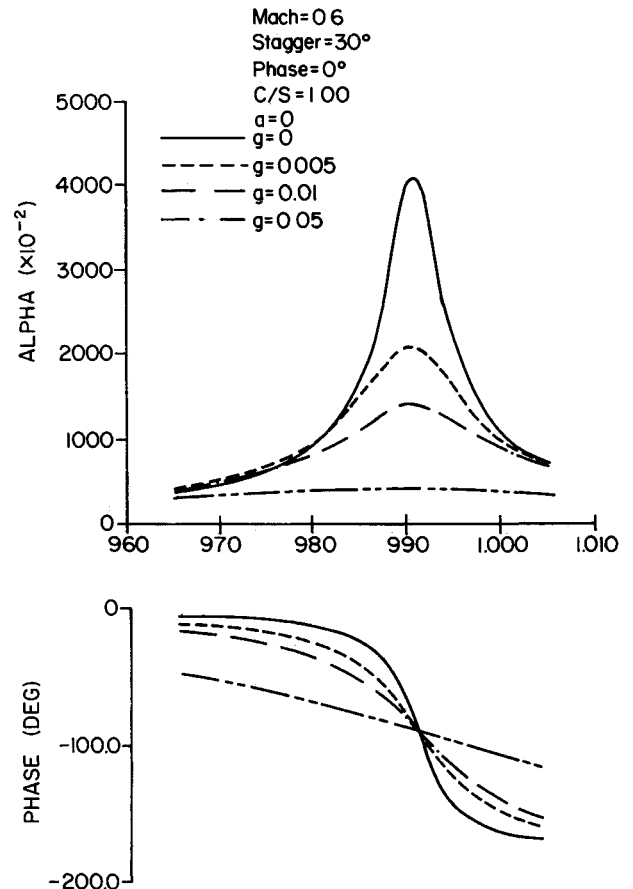


Fig 3 Structural damping effect on the coupled torsional response amplitude for $(\bar{\omega}/\omega_\alpha)$ near ω_α

The energy dissipated by the structural damping over one cycle of oscillation can be calculated as follows

$$\begin{aligned} (\text{WORK})_{g_h}^h &= \oint \text{Re}[ig_h m \omega_h^2 h dh] = \pi g_h m \omega_h^2 h_0^2 \\ (\text{WORK})_{g_\alpha}^\alpha &= \oint \text{Re}[ig_\alpha I_\alpha \omega_\alpha^2 \alpha d\alpha] = \pi g_\alpha I_\alpha \omega_\alpha^2 \alpha_0^2 \end{aligned} \quad (8)$$

The unsteady work associated with the static moment S_α merits some additional comment. This is the term which couples the system equations of motion when the elastic axis and the aerodynamic center do not coincide. Physically the S_α term can be considered as either a torsional force applied to the airfoil as the result of a unit translation airfoil displacement or as a translational force resulting from the application of a unit torsional displacement. Thus, for an airfoil undergoing a translation mode oscillation, there is an apparent torsional load that can either do work on or extract work from the airfoil system. The phase relationship between the translational and torsional displacement determines whether this apparent torsional load adds or dissipates energy in the airfoil system.

The unsteady work per cycle of oscillation associated with the static moment can be determined by Eq. (9)

$$\begin{aligned} (\text{WORK})_{S_\alpha}^h &= \oint \text{Re}[S_\alpha \ddot{\alpha} dh] = S_\alpha \bar{\omega}^2 \alpha_0 h_0 \pi \sin(\lambda_h - \lambda_\alpha) \\ (\text{WORK})_{S_\alpha}^\alpha &= \oint \text{Re}[S_\alpha \dot{h} d\alpha] = S_\alpha \bar{\omega}^2 \alpha_0 h_0 \sin(\lambda_\alpha - \lambda_h) \end{aligned} \quad (9)$$

The substitution of the various work expressions into the energy balance [see Eq. (4)] yields the following matrix expression for the coupled translational and torsional airfoil displacements

$$\begin{bmatrix} A_{11} & A_{12} \\ A_{21} & A_{22} \end{bmatrix} \begin{bmatrix} \left(\frac{h_0}{b}\right) \\ (\alpha_0) \end{bmatrix} = \begin{bmatrix} B_{11} \\ B_{21} \end{bmatrix} \quad (10)$$

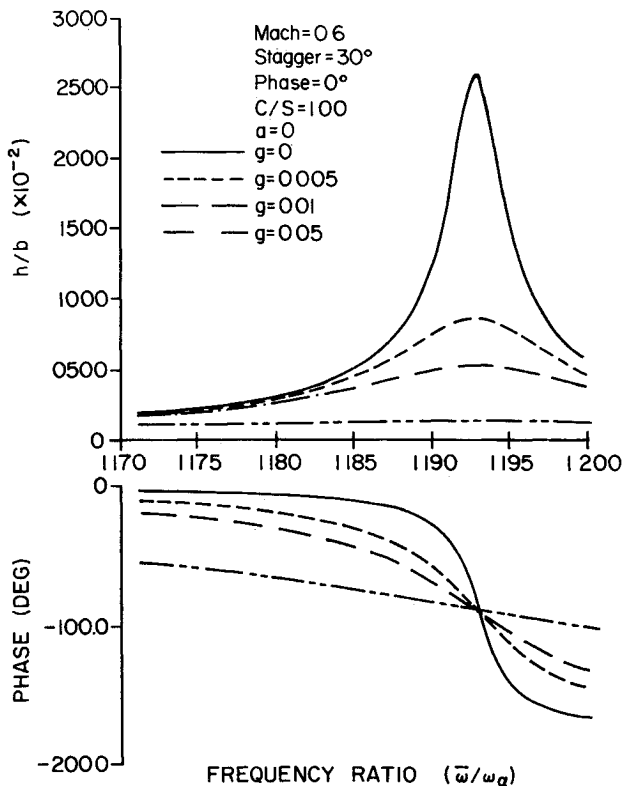


Fig. 4 Structural damping effect on the coupled torsional response for $(\bar{\omega}/\omega_\alpha)$ near ω_h

where

$$\begin{aligned} A_{11} &= [\pi g_h m \omega_h^2 b] + [(A_h)^1 \pi^2 \rho b^3 \bar{\omega}^2] \\ A_{12} &= [S_\alpha \bar{\omega}^2 \pi - (A_\alpha)^R \pi^2 \rho b^3 \bar{\omega}^2] \sin(\lambda_h - \lambda_\alpha) \\ &\quad + [(A_\alpha)^1 \pi^2 \rho b^3 \bar{\omega}^2 \cos(\lambda_h - \lambda_\alpha)] \\ A_{21} &= [S_\alpha \bar{\omega}^2 \pi - (B_h)^R \pi^2 \rho b^4 \bar{\omega}^2] \sin(\lambda_\alpha - \lambda_h) \\ &\quad + [(B_h)^1 \pi^2 \rho b^4 \bar{\omega}^2 \cos(\lambda_h - \lambda_\alpha)] \\ A_{22} &= \pi g_\alpha I_\alpha \omega_\alpha^2 + (B_\alpha)^1 \pi \rho b^4 \bar{\omega}^2 \\ B_{11} &= -\pi \rho b^3 \bar{\omega}^2 \left(\frac{W_G}{U}\right) [(A_G)^1 \cos(\lambda_h) - (A_G)^R \sin(\lambda_h)] \\ B_{21} &= \pi^2 \rho b^4 \bar{\omega}^2 \left(\frac{W_G}{U}\right) [(B_G)^1 \cos(\lambda_\alpha) - (B_G)^R \sin(\lambda_\alpha)] \end{aligned}$$

The phase angles between the translational and torsional displacements, λ_h and λ_α respectively, can be determined in various ways. For example, they can be determined directly from the classical solution of the coupled system equations of motion Eq. (3) (see Ref. 5). For convenience and brevity these phase angle relationships are presented in Eq. (11)

$$\begin{aligned} \lambda_h &= \tan^{-1} \left[\frac{N_{hI} D_R - N_{hR} D_I}{N_{hR} D_R + N_{hI} D_I} \right] \\ \lambda_\alpha &= \tan^{-1} \left[\frac{N_{\alpha I} D_R - N_{\alpha R} D_I}{N_{\alpha R} D_R + N_{\alpha I} D_I} \right] \end{aligned} \quad (11)$$

where N_{hI} , $N_{\alpha I}$, N_{hR} , $N_{\alpha R}$, D_R , and D_I are defined in terms of the airfoil structural properties and the unsteady aerodynamic forces and moments in the Nomenclature.

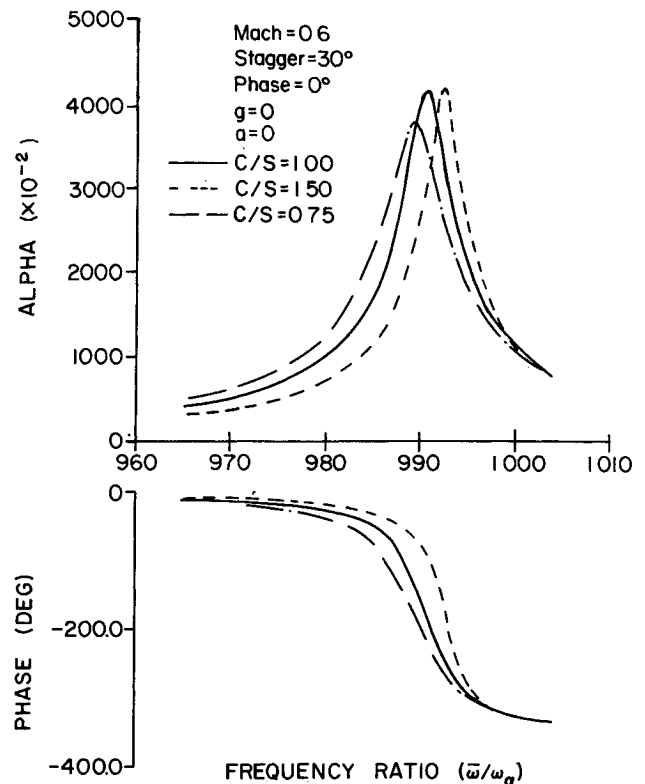


Fig. 5 Cascade solidity effect on the coupled torsional response

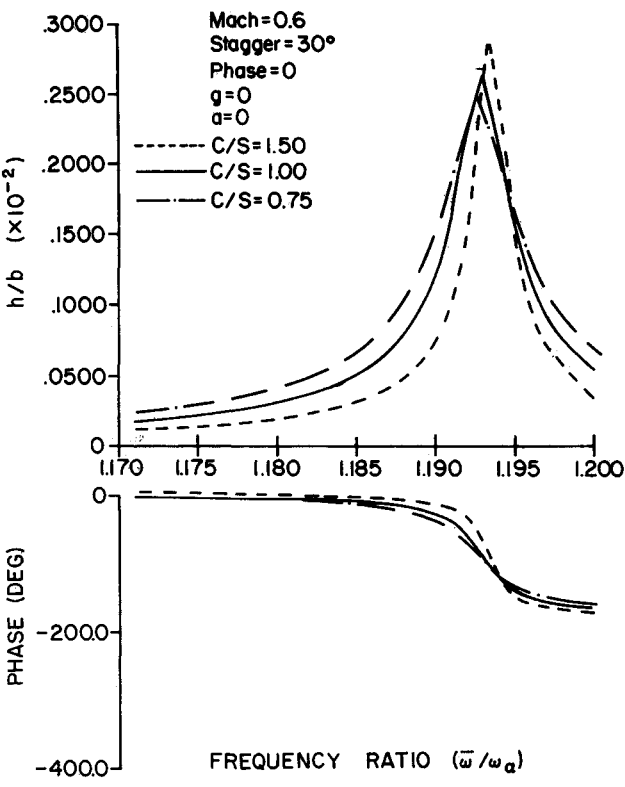


Fig. 6 Cascade solidity effect on the coupled translational response.

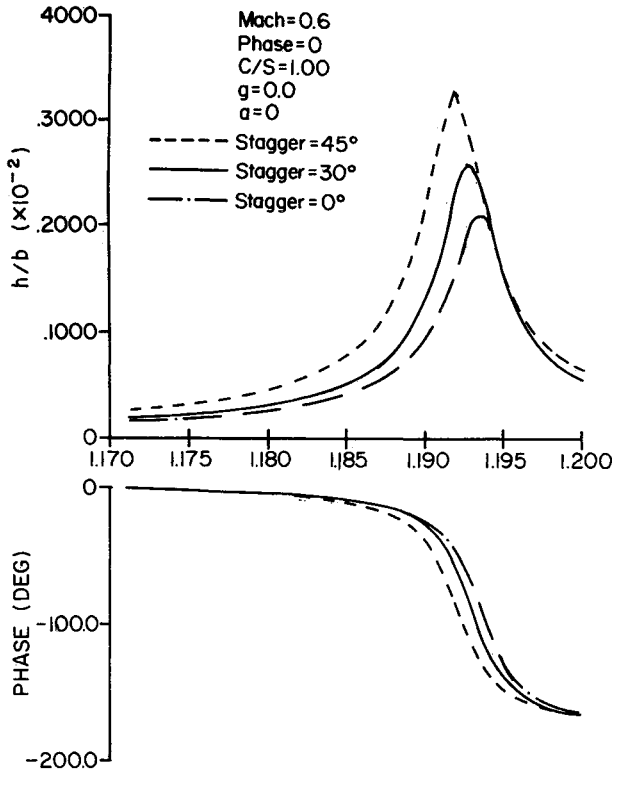


Fig. 8 Effect of stagger angle on the coupled translational response.

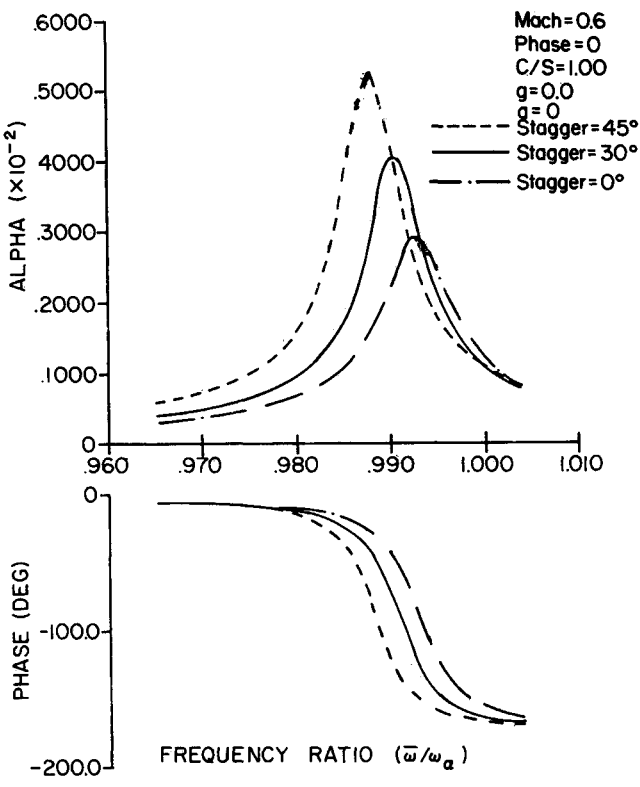


Fig. 7 Effect of stagger angle on the coupled torsional response.

Unsteady Aerodynamic Forces and Moments

L_h , M_h , L_α and M_α denote the standard form for the unsteady aerodynamic forces and moments and represent the unsteady lift and moment in translation and torsion, respectively calculated about the airfoil $\frac{1}{4}$ chord. These standard form $\frac{1}{4}$ chord coefficients are related to the general unsteady aerodynamic influence coefficients through the following relationships

$$\begin{aligned} A_h &= L_h \\ A_\alpha &= L_\alpha - (\frac{1}{2} + a)L_h \\ A_G &= L_w \\ B_h &= M_h - (\frac{1}{2} + a)L_h \\ B_\alpha &= M_\alpha - (\frac{1}{2} + a)(L_\alpha + M_h) + (\frac{1}{2} + a)^2 L_h \\ B_G &= M_w \end{aligned} \tag{12}$$

where a is the dimensionless distance of the elastic axis measured from the airfoil mid-chord (see Fig. 1).

Results

To demonstrate the effects of the various parameters on the coupled forced response of turbomachinery blading, the unsteady aerodynamic analysis of Ref. 7 will be utilized. This analysis predicts the gust and self-induced unsteady aerodynamic forces and moments in a compressible flow field. The structural properties for this parametric study are based on an airfoil with a 5.08-cm chord, a 4% thickness-to-chord ratio, and an aspect ratio of 3. This representative airfoil has a natural translation mode frequency, ω_h , 12% larger than the natural torsion mode frequency, ω_α . Hence, $\omega_h/\omega_\alpha = 1.12$. Specific parameters to be varied include the structural damping value, the cascade solidity, the interblade phase angle, the inlet Mach number, and the elastic axis location. In addition, to clearly demonstrate the coupling effects, the airfoil stiffness is varied so as to make the torsional and translation mode natural frequencies nearly equal in value.

To verify the energy-balance approach for the prediction of aerodynamically-induced vibrations, the uncoupled torsion mode response of the representative airfoil was calculated by means of both the energy balance technique and a classical Newton's second law approach.⁵ Figure 2 presents the comparison of these calculation techniques. As shown, the two methods yield identical results, both in terms of the amplitude and the phase of the response.

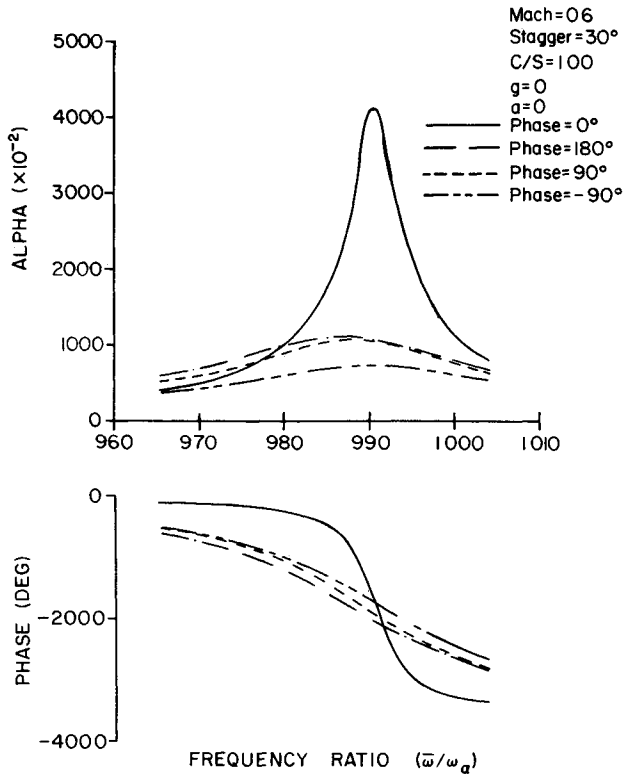


Fig 9 Effect of interblade phase angle on the coupled torsion mode response

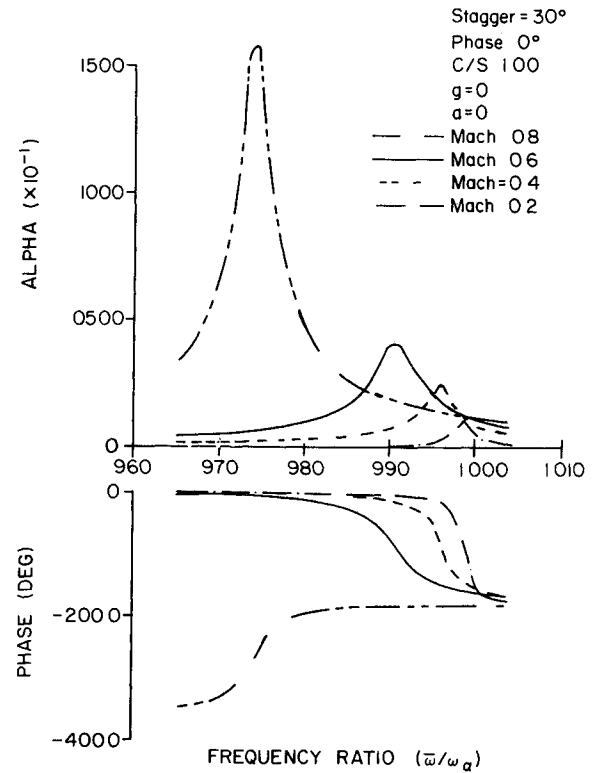


Fig 11 Inlet Mach number effect on the coupled torsional response

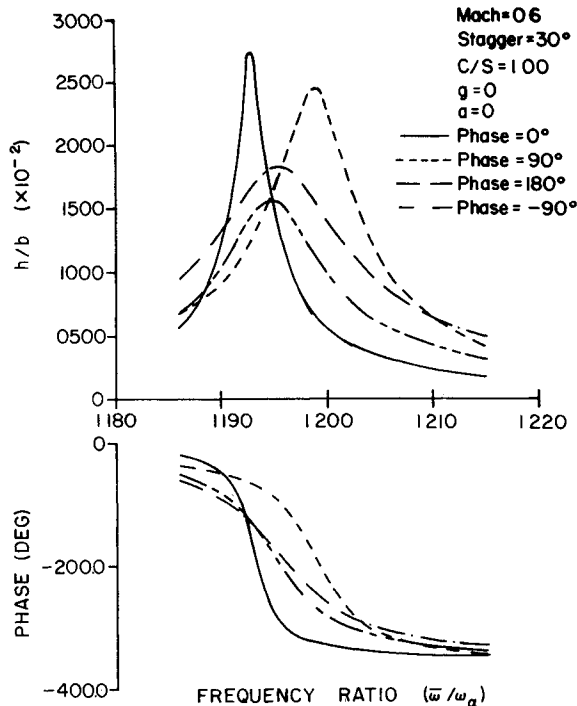


Fig 10 Effect of interblade phase angle on the coupled translation mode response

The coupled forced response characteristics of the representative airfoil are determined utilizing this energy balance technique. Results are presented as a function of the nondimensional ratio of the gust forcing frequency to the airfoil natural torsion mode frequency $\bar{\omega}/\omega_\alpha$. Hence values of 1.00 and 1.12 for this nondimensional frequency ratio correspond to the situations where the forcing function frequency is equal to the natural torsion and translation mode

frequencies respectively of the representative airfoil. Results presented include the translational amplitude, the torsion mode amplitude, and the phase angles between the aerodynamic forcing function and the resulting airfoil response as a function of the nondimensional frequency ratio.

As anticipated, when the gust forcing function frequency is close to the natural torsion mode frequency, the torsional response is an order of magnitude greater than the corresponding coupled translation mode response. Thus, only the coupled forced torsional response will be presented for the forcing function close to the airfoil natural torsional frequency ($\bar{\omega}/\omega_\alpha \approx 1.00$) and only the coupled forced translational response for forcing function frequencies near the natural translational frequency ($\bar{\omega}/\omega_\alpha \approx 1.12$) will be presented.

Figures 3 and 4 represent the torsional and translational airfoil responses, respectively, with structural damping as the parameter when the forcing frequency is close to ω_α and ω_h , respectively. As seen, increased structural damping resulting in decreased amplitude of response. It should be noted that the maximum response amplitudes do not occur at frequency ratio values of 1.00 and 1.12, even for the special case of zero structural damping. This is a result of the self-induced unsteady aerodynamic forces which correspond in this case to aerodynamic damping. Thus, even when there is no structural damping in the airfoil system, the self-induced aerodynamics generate aerodynamic damping.

The effects of cascade solidity (C/S) and stagger angle on the coupled forced response amplitudes are demonstrated in Fig 5 and 6 and Figs 7 and 8, respectively. Both the coupled torsional and translational forced response amplitudes increase with increasing values for solidity and stagger angle. Variations in solidity result in a somewhat more pronounced effect on the translational response than on the torsional response. Stagger angle variation has a greater effect on the torsional response than on the translational one. Also, variations in stagger angle have a much greater effect on the response amplitudes, both torsional and translational, than do variations in solidity. It should be noted that the design trend for modern compressors includes increased solidity and

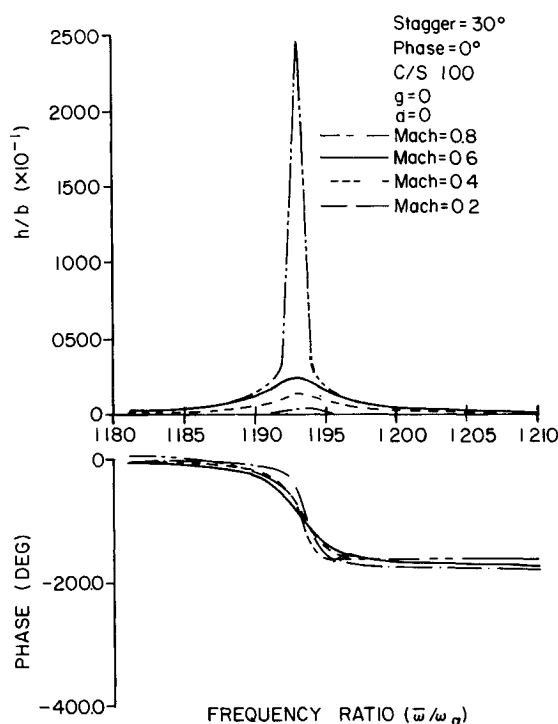


Fig 12 Inlet Mach number effect on the coupled translational response

stagger angle values. Hence these results indicate that in creased forced response problems primarily associated with increased stagger angles might be anticipated.

Figures 9 and 10 show the effect of interblade phase angle on the coupled airfoil forced response characteristics. The effect of variations in this parameter on the coupled torsional forced response are quite different than on the coupled translational response. For the torsion mode there is only an extreme maximum response amplitude for a 0 deg interblade phase angle value. For all other values considered the response amplitude curves are relatively flat and decreased from the 0 deg case by approximately 75 to 85%. The coupled translational response amplitudes all exhibit an extreme maximum response amplitude i.e. none of the amplitude response curves are relatively flat. Also although an interblade phase angle value of 0 deg results in the maximum forced translational response amplitude varying the interblade phase angle away from 0 deg results in noticeably smaller decreases in this maximum amplitude than were noted for the forced torsional response. In particular for both the torsional and the translational cases the largest decrease in the maximum response amplitude is associated with changing the interblade phase angle value from 0 to -90 deg. However the maximum forced translational response decreased only 45% whereas the corresponding forced torsional response decreased by 85%. In addition since the smallest coupled torsional and translational response amplitudes correspond to negative interblade phase angle values (-90 deg in particular) then this would appear to be a desirable forced response design condition. In terms of the rotor stator interaction forced response problem a negative interblade phase angle value corresponds to a backward traveling wave as viewed from the stator vane frame of reference and arises when the number of rotor blades is greater than the number of stator vanes.

The effect of the inlet flow Mach number on the coupled torsional and translational forced response characteristics of the representative airfoil is demonstrated in Figs 11 and 12 respectively. Increasing the Mach number which also corresponds to decreasing the reduced frequency for a specific

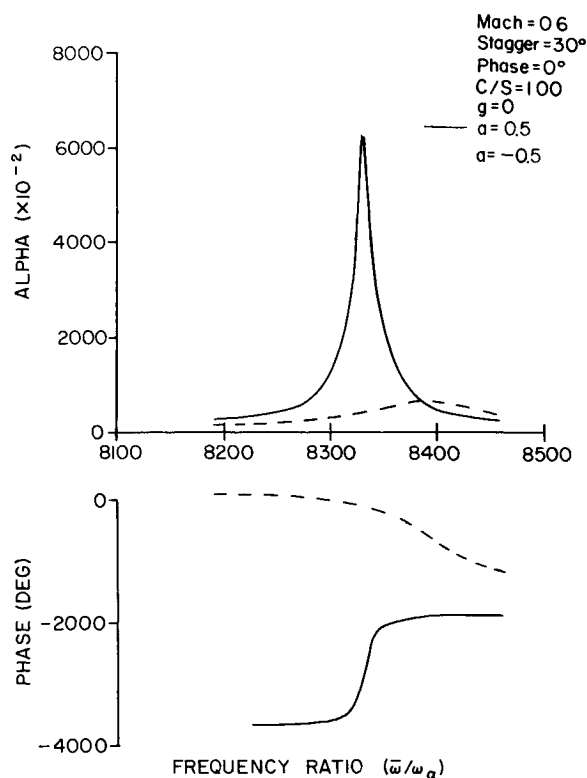


Fig 13 Effect of elastic axis location on the coupled torsional response for ($\bar{\omega}/\omega_\alpha$) near ω_α

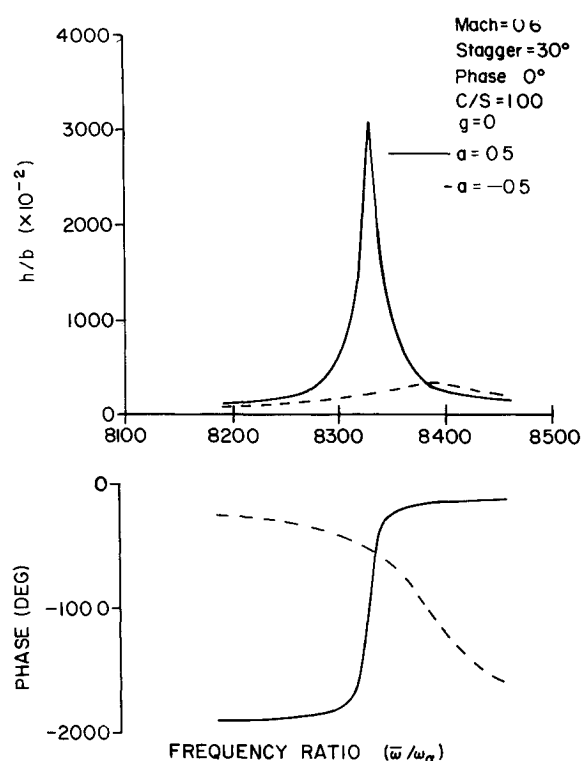


Fig 14 Effect of elastic axis location on the coupled translational response for ($\bar{\omega}/\omega_\alpha$) near ω_α

gust disturbance increases both the coupled torsional and translational responses with a very dramatic increase associated with an increase in Mach number from 0.6 to 0.8. Also for Mach numbers of 0.6 and smaller the increase in the maximum response amplitude is much larger for the torsional mode than for the translational mode. In addition the forcing

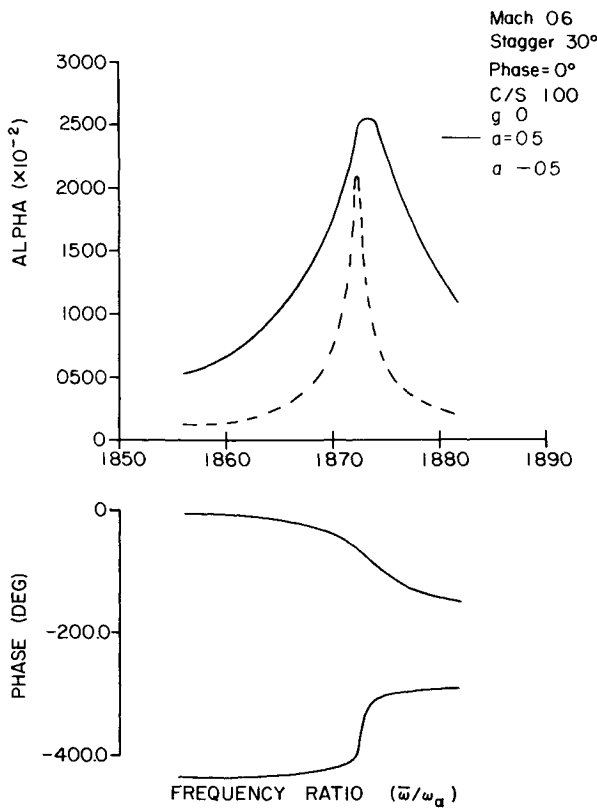


Fig 15 Effect of elastic axis location on the coupled torsional response for $(\bar{\omega}/\omega_\alpha)$ near ω_h

function frequency at which the maximum amplitude response occurs is highly dependent on the Mach number for the torsional response but is almost independent of this forcing frequency for the translational response case

The effect of moving the elastic axis location to the $1/4$ chord and the $3/4$ chord locations on the coupled forced response of the representative airfoil is presented in Figs 13 through 16. These results indicate that not only the response amplitude but also the forcing function frequency at which the maximum amplitude response occurs is strongly dependent on the position of the elastic axis. The maximum torsion and translation response amplitudes are found with the elastic axis at the $3/4$ chord location. Shifting the elastic axis forward to the $1/4$ chord location results in significantly decreasing both the torsional and translational response amplitudes near the airfoil torsional natural frequency but only slightly decreasing these response amplitudes near the airfoil translational natural frequency. Also shifting the elastic axis location aft from mid chord to $3/4$ chord has the result of making the translational response in the neighborhood of the natural torsional frequency ($\bar{\omega}/\omega_\alpha \approx 1.0$) the same order of magnitude as the torsional response amplitude, indicating the significant additional coupling that arises when the elastic axis and the airfoil center of gravity do not coincide. Similar results are noted when the forcing function frequency is close to the natural translational frequency.

To demonstrate the interaction of two very closely spaced torsional and translation modes the bending stiffness of the representative airfoil was altered to make the ratio of translation to torsion natural frequencies 1.02. The variation with interblade phase angle values of these closely coupled forced torsional and translational responses was then investigated. The results are presented in Figs 17 and 18. The coupled torsional response results (Fig 17) show that at a frequency ratio of 0.990 the response decreases as the interblade phase angle is varied from 0 to $+90^\circ$, -90° and 180° . At a frequency ratio of 1.015 the response increases by up to 65%.

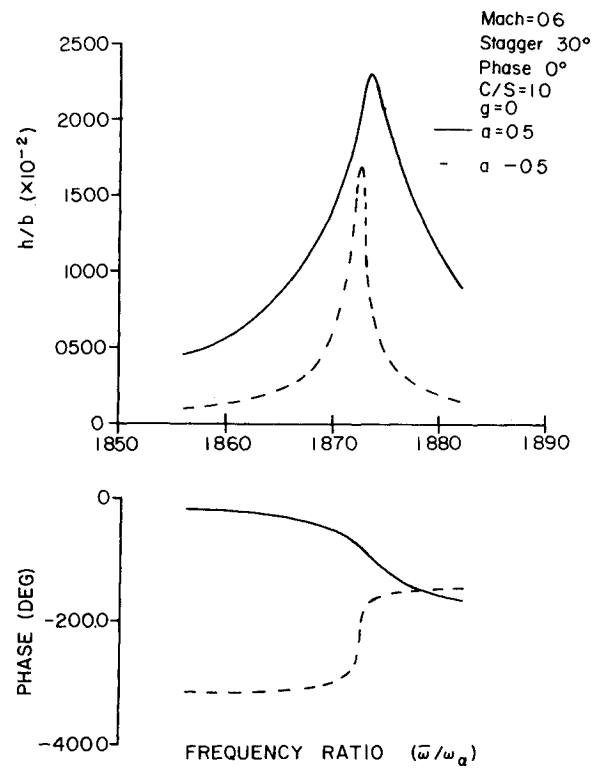


Fig 16 Effect of elastic axis location on the coupled translational response for $(\bar{\omega}/\omega_\alpha)$ near ω_h

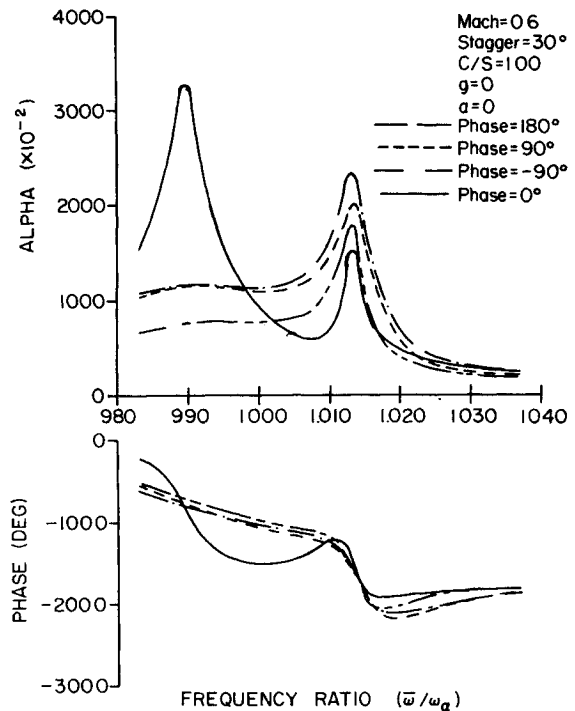


Fig 17 Interblade phase angle effect on the coupled torsional response for nearly equal natural frequencies

Figure 18 presents the variation of the forced translational response with the interblade phase angle as the parameter. In contrast to the torsional response results, minimal translational response is noted when the forcing function frequency is near the airfoil natural torsional frequency. However, when the forcing function frequency is near the airfoil natural translational frequency ($\bar{\omega}/\omega_\alpha \approx 1.015$) the

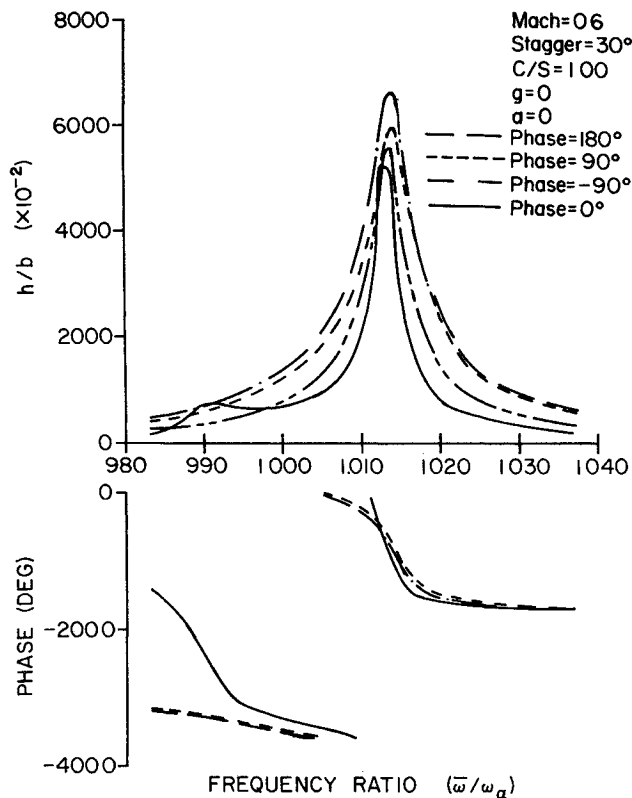


Fig 18 Interblade phase angle effect on the coupled translational response for nearly equal natural frequencies

forced translational amplitude is significant and increases as the interblade phase angle value is varied from 0 to 180 deg. A comparison of Figs 17 and 18 at a frequency ratio close to 1.015 reveals a correspondence between the forced torsional response and the translational one. This is caused by the high degree of coupling that exists between the translational and torsional modes for the altered airfoil.

Summary and Conclusions

In this investigation the coupled structural dynamic airfoil system forced response was determined utilizing an energy balance technique. The energy input to the system per cycle of oscillation was generated by the gust and under certain conditions, the self-induced aerodynamic forces and moments. The energy dissipation per cycle of oscillation was associated with system structural damping under some conditions the self-induced aerodynamic forces and moments and the static moment term S_α . It should be noted that for the uncoupled single degree of freedom case the dissipative coupling mechanism S_α is not considered.

The effects of the various aerodynamic parameters on the coupled translational and torsional mode forced response of a representative airfoil were then considered. The study showed the increased coupling between the torsion and translation modes as the corresponding undamped natural frequencies approach one another. It was also demonstrated that the coupled torsional and translational forced response amplitudes of a representative airfoil increased with: 1) decreased structural damping 2) increased solidity values 3) increased stagger angles 4) increased inlet flow Mach numbers 5) interblade phase angle values corresponding to forward traveling waves for the rotor stator interaction case and 6) shifting of the elastic axis location aft.

It should be noted that variations in the above parameters did not affect the magnitude of the resulting forced response equally nor did they always have equivalent effects on the torsional and translational response modes. For example, increasing the stagger angle and shifting the elastic axis aft resulted in significantly larger increases in all of the response amplitudes than did increasing the solidity. Also, the interblade phase angle, for example, had a much greater effect on the coupled torsion mode responses than on the translational ones. In addition, the forcing function frequencies at which the maximum torsional and translational responses occurred did not generally correspond to the airfoil natural torsional or translational frequencies. This was because the self-induced aerodynamic forces and moments result in an aerodynamic damping effect analogous to structural damping.

Acknowledgment

The Air Force Office of Scientific Research and Capt Michael Francis, who served as the project's technical monitor, are gratefully acknowledged for their support.

References

- ¹ The Aerothermodynamics of Aircraft Gas Turbine Engines AFAPL TR 78-52, July 1978.
- ² Fleeter, S., Jay, R. L., and Bennett, W. A., Rotor Wake Generated Unsteady Aerodynamic Response of a Compressor Stator, *ASME Journal of Engineering for Power*, Vol. 100, No. 4, Oct. 1978, pp. 664-675.
- ³ Fleeter, S., Aeroelasticity Research for Turbomachine Application, *Journal of Aircraft*, Vol. 16, May 1979, pp. 320-326.
- ⁴ Platzer, M. F., Unsteady Flows in Turbomachines—A Review of Recent Developments, AGARD CP 227, Sept. 1977.
- ⁵ Fung, Y. C., *An Introduction to the Theory of Aeroelasticity*, Dover Publications, New York, N.Y., 1969.
- ⁶ Hoyniak, D., and Fleeter, S., Prediction of Aerodynamically Induced Vibrations in Turbomachinery Blading, *ASME Symposium in Fluid/Structure Interaction in Turbomachinery*, Nov. 1981.
- ⁷ Fleeter, S., The Fluctuating Lift and Moment Coefficients for Cascaded Airfoils in a Nonuniform Compressible Flow, *Journal of Aircraft*, Vol. 10, Feb. 1973, pp. 93-98.